

Supporting Information

Towards “Green” Electronic Materials. α -Oligofurans as Semiconductors

Ori Gidron,[†] Afshin Dadvand,[§] Yana Sheynin,[†] Michael Bendikov,^{†*} and Dmitrii F. Perepichka^{§*}

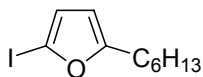
[†] Department of Organic Chemistry, Weizmann Institute of Science, Rehovot 76100, Israel and

[§] Department of Chemistry, McGill University, 801 Sherbrooke Street West, Montreal, Quebec, Canada H3A 2K6

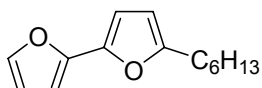
General Information

^1H and ^{13}C NMR spectra were recorded in solution on a 300 MHz spectrometer (Brücker) using ^2H -chloroform as the solvent and tetramethylsilane (TMS) as the external standard. Chemical shifts are expressed in δ units. High resolution mass spectra were measured on a Waters Micromass GCT_Premier Mass Spectrometer using field desorption (FD) ionization. Differential scanning calorimetry (DSC) measurements were performed on a TA Q200 DSC instrument. Thermogravimetric analysis (TGA) measurements were performed on a TA Q600 instrument. UV-vis absorption measurements were made on a Cary-50 spectrometer (Varian). Steady state fluorescence measurements were performed on a Cary Eclipse fluorimeter (Varian) with the excitation/emission geometry at right angles. Fluorescence quantum yields (Φ_f) were determined using a standard procedure,¹ and coumarine 30 in MeCN ($\lambda_{\text{abs}} = 403 \text{ nm}$, $\lambda_{\text{em}} = 480 \text{ nm}$, $\Phi_f = 0.67$) was used as a reference.² Quantum yield measurements were made using four excitation wavelengths, the quantum yields were averaged over 20 measurements, and the errors were estimated to be less than 5%. XRD measurements of oligofuran films on Si/SiO₂ slides and as powders were performed on an XRD diffractometer (TTRAXIII, Japan). AFM topography images of oligofuran films on Si/SiO₂ slides were acquired using a P47 AFM (NT-MDT) equipped with a small scanner. Images were recorded in tapping mode in the air at room temperature (22–25 °C) using silicon micro cantilevers (OMCL-AC240TS-W2, Olympus). The set point ratio was adjusted to 0.75–0.8 (corresponding to “light” tapping). Dichloroethane (DCE) containing 0.1 M tetra-*n*-butylammonium tetrafluoroborate (TBABF₄) was used as a solvent. Ag/AgCl was used as a reference electrode. A ferrocene/ferrocenium redox couple ($\text{Fc}/\text{Fc}^+ = 0.40 \text{ V}$ vs. saturated calomel electrode (SCE) in DCE)³ was used as an internal reference for all measurements. All electrochemical measurements were performed under a dry nitrogen atmosphere. Dry anhydrous DCE was purchased from Sigma-Aldrich and used as it is. TBABF₄ (Fluka) was dried under vacuum. Ferrocene powder (Fluka) was used to establish an electrochemical reference. Ag/AgCl wire was prepared by dipping silver wire in a solution of FeCl₃ and HCl. Tetrahydrofuran (THF) and toluene were distilled from sodium/benzophenone

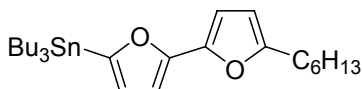
under an atmosphere of dry argon prior to use. Columns were prepared with silica gel (60-230 mesh). The syntheses of **8F** and **6F** has been described elsewhere.⁴



2-hexyl-5-iodofuran (1). A solution of *n*-BuLi (24.7 mL, 1.6 M in hexanes, 39.5 mmol, 1.4 equivalents) was added dropwise to a solution of 2-hexylfuran (4.3 g, 28.3 mmol) in dry THF (50 mL) at -78°C under N₂. The reaction mixture was warmed to 0°C, stirred for 10 min and cooled again to -78°C. Iodine (9.3 g, 36.7 mmol) in 25 mL of THF was slowly added to this solution, which was warmed slowly to 0°C and stirred for 2 h. After the addition of 100 mL of water, the solution was extracted with hexane. The organic layer was washed with aqueous Na₂S₂O₃ solution (30 mL) and water, dried over MgSO₄, filtered, and concentrated. The crude product was purified by silica gel column chromatography (elution with hexane) to afford 6 g of **1** (76%) as a pale brownish oil. ¹H NMR (300 MHz, CDCl₃): δ 86.37 (d, *J* = 3.14 Hz, 1H), 5.88 (d, *J* = 3.16 Hz, 1H), 2.60 (t, *J* = 7.56, 7.56 Hz, 2H), 1.58 (td, *J* = 15.11, 7.66, 7.66 Hz, 2H), 1.24-1.39 (m, 6H), 0.86 (t, *J* = 6.77, 6.77 Hz, 3H) ppm. ¹³C NMR (75 MHz, CDCl₃): δ 162.3, 120.6, 108.0, 84.3, 31.6, 28.8, 28.3, 27.8, 22.6, 14.1 ppm.

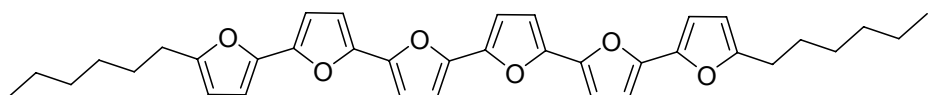


5-hexyl-2,2'-bifuran (2). Pd(PPh₃)₄ (1.15 g, 1 mmol, 5 % mol) was added to 2-tributyltinfuran (7.05 g, 20 mmol) and **1** (5.5 g, 20 mmol) in dry toluene (150 mL) and the reaction mixture was refluxed under N₂ for 5 h. The mixture was then cooled, separated with hexane, the organic layer was dried over MgSO₄, filtered, and concentrated. The crude product was purified by silica gel column chromatography (elution with hexane) to afford 3.8 g of **2** (88%) as a colorless oil. ¹H NMR (300 MHz, CDCl₃): δ 7.35 (d, *J* = 1.1 Hz, 1H), 6.39-6.45 (m, 3H), 6.00 (d, *J* = 3.2 Hz, 1H), 2.62 (t, *J* = 7.6, 2H), 1.64 (td, *J* = 2H), 1.28-1.34 (m, 6H), 0.87 (t, 3H) ppm. ¹³C NMR (75 MHz, CDCl₃): δ 156.3, 147.0, 144.8, 141.3, 111.3, 106.5, 105.9, 104.1, 31.6, 28.9, 28.1, 28.0, 22.6, 14.1 ppm.



tributyl(5'-hexyl-[2,2'-bifuran]-5-yl)stannane (3). A solution of *n*-BuLi (14.1 mL, 1.6 M in hexanes, 22.5 mmol, 1.3 equivalents) was added dropwise to a solution of **2** (3.8 g, 17.4 mmol) in dry tetrahydrofuran (THF, 100 mL) at -78°C under N₂. The reaction mixture was allowed to reach room temperature and stirred for 1 h. The resulting mixture was cooled to -78°C, Bu₃SnCl (6.1 mL, 22.5 mmol) was added dropwise, and the reaction mixture was allowed to reach room temperature and stirred for 2 h. The mixture was quenched with water, extracted with hexane, dried (MgSO₄), and evaporated. Flash chromatography on basified (NEt₃) silica, using hexane as

eluent gave **3** (1.9 g, 20% yield) as a colorless oil. ¹H NMR (300 MHz, CDCl₃): δ 6.61 (d, *J* = 3.31 Hz, 1H), 6.53 (d, *J* = 2.76 Hz, 1H), 6.46 (d, *J* = 2.76 Hz, 1H), 6.07 (d, *J* = 3.31 Hz, 1H), 2.69 (t, *J* = 7.17, 2H), 1.58-1.72 (m, 8H), 1.31-1.45 (m, 14H) 1.13 (m, 4H), 0.92-0.97 (m, 12H).ppm. ¹³C NMR (75 MHz, CDCl₃): δ 106.1, 155.9, 151.4, 145.7, 122.9, 106.4, 105.4, 104.0, 31.6, 28.9, 28.8, 28.1, 28.0, 27.2 22.6, 14.7, 14.1, 10.2 ppm. HRMS (FD): *m/z* calcd for C₂₆H₄₄O₂Sn: 508.2368; found 508.2374.



5,5''''-dihexyl-2,2':5',2'':5'',2''''-sexifuran (DH-6F). Pd(PPh₃)₄ (115 mg, 0.1 mmol, 5 % mol) was added to 2,5'-(dibromo)bisfuran (283 mg, 1 mmol) and **3** (1 g, 2 mmol) in dry toluene (200 mL) and the reaction mixture was refluxed under N₂ for 5 h. The mixture was then cooled, concentrated to approximately 50 mL, the residue was collected by filtration, washed with acetone, and sublimed under reduced pressure (10⁻² mbar) at 190–200°C to give 190 mg of **DH-6F** (35 % yield) as a bright yellow powder, m.p. 261°C. ¹H NMR (400 MHz, 1,1,2,2-tetrachloroethane-d₂, 60°C): δ 6.68 – 6.61 (m, 6H), 6.52 (d, *J* = 3.6 Hz, 2H), 6.50 (d, *J* = 3.2 Hz, 2H), 6.03 (d, *J* = 3.3 Hz, 2H), 2.64 (t, *J* = 7.5 Hz, 4H), 1.64 (dt, *J* = 15.1, 7.4 Hz, 4H), 1.39 – 1.25 (m, 12H), 0.86 (t, *J* = 7.0 Hz, 6H). ¹³C NMR (100 MHz, 1,1,2,2-Tetrachloroethane-d₂, 60°C): δ 157.3, 145.8, 145.1, 144.6, 107.9, 107.6, 107.1, 106.6, 31.6, 29.9, 29.0, 28.2, 22.7, 14.1 ppm. HRMS (FD): *m/z* calcd for C₃₆H₃₈O₆: 566.2668; found 566.2674.

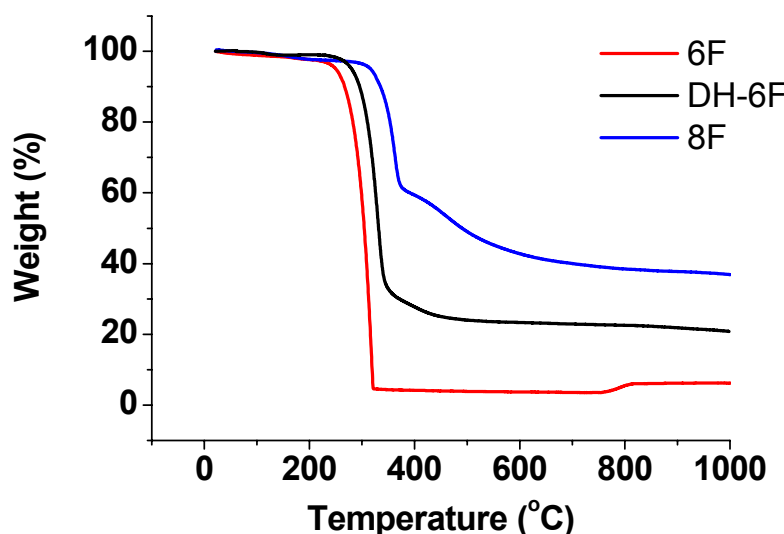


Figure S1: Thermogravimetric analysis (TGA) of oligofurans under N₂. Rate: 5°C/min.

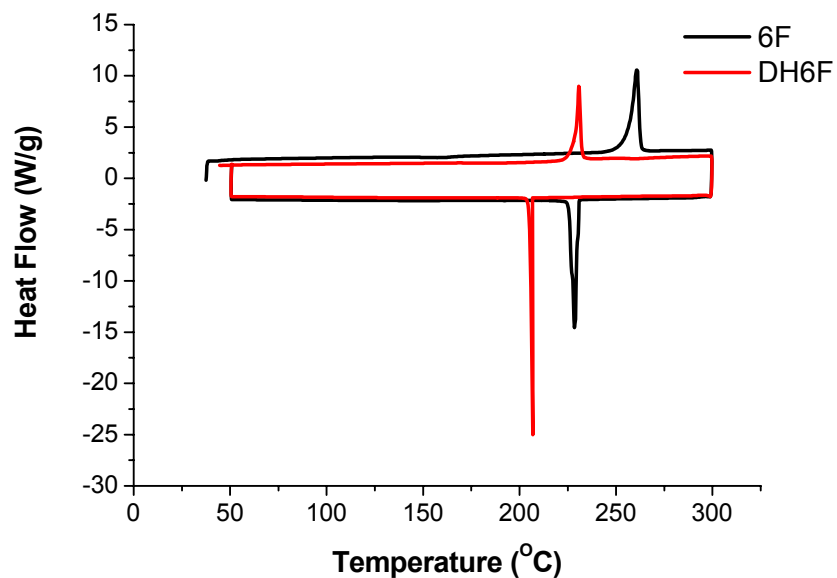


Figure S2: Differential scanning calorimetry (DSC) of oligofurans under N₂, rate: 5°C/min.

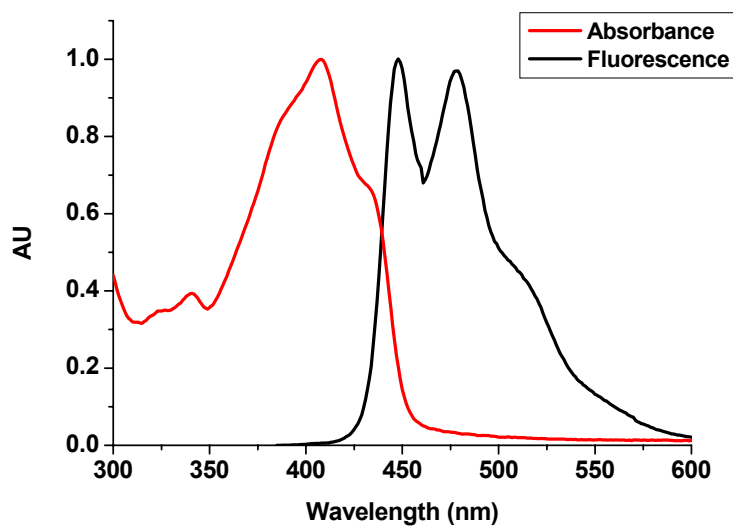


Figure S3. Normalized absorbance (red) and fluorescence (black) spectra of **DH-6F** in dioxane.

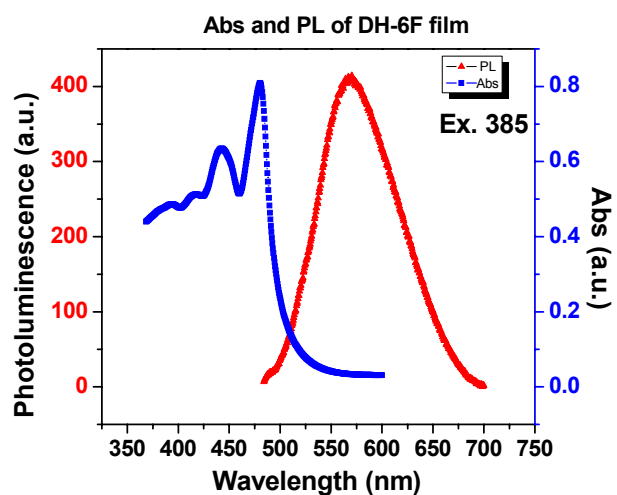


Figure S4. Absorbance (blue) and photoluminescence (PL; red) spectra of a 50 nm thick film of vacuum sublimed **DH-6F** on glass a substrate (deposition rate=3 Å/s).

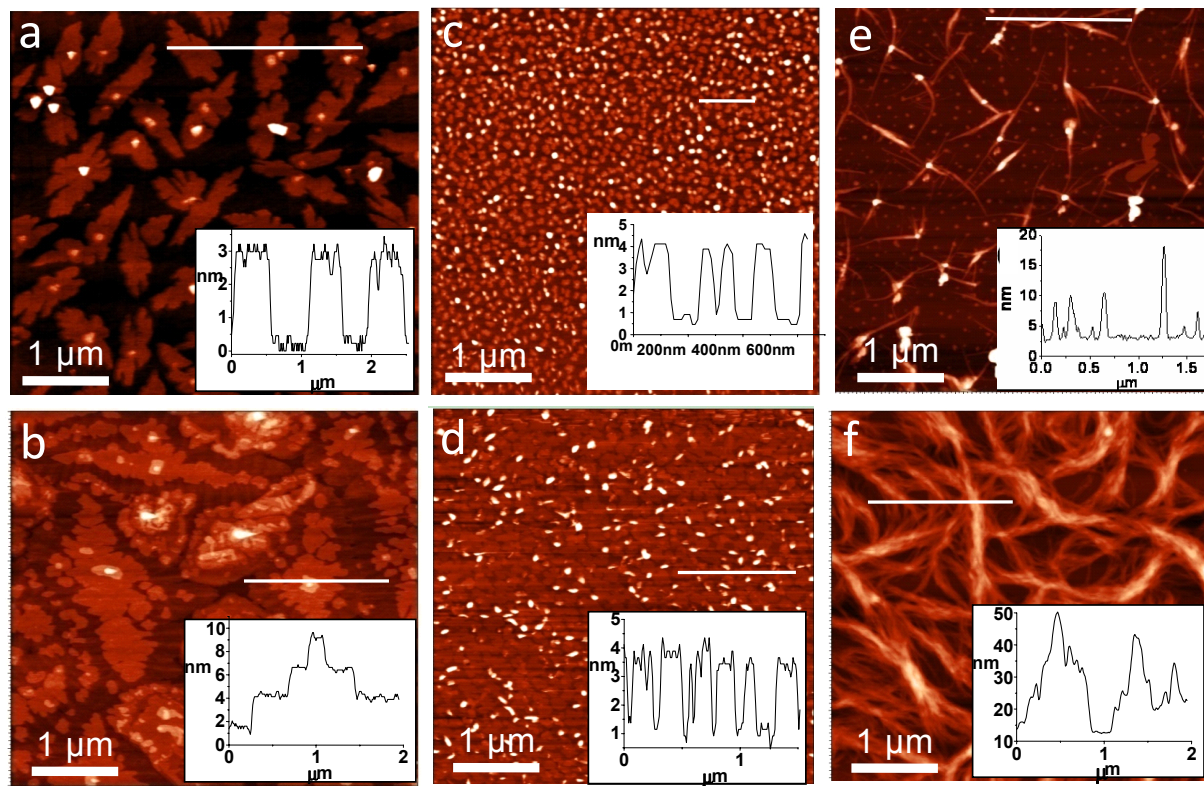


Figure S5. AFM images and cross section diagrams of (a) **DH-6F** after a deposition time of 20 s (sub-monolayer regime), (b) **DH-6F** after a 120 s deposition time (thickness of 3 layers), (c) **8F** after a deposition time of 20 s, (d) **8F** after a deposition time of 60 s, (e) **6F** after a deposition time of 20 s, and (f) **6F** after a deposition time of 60 s, on Si/SiO₂.

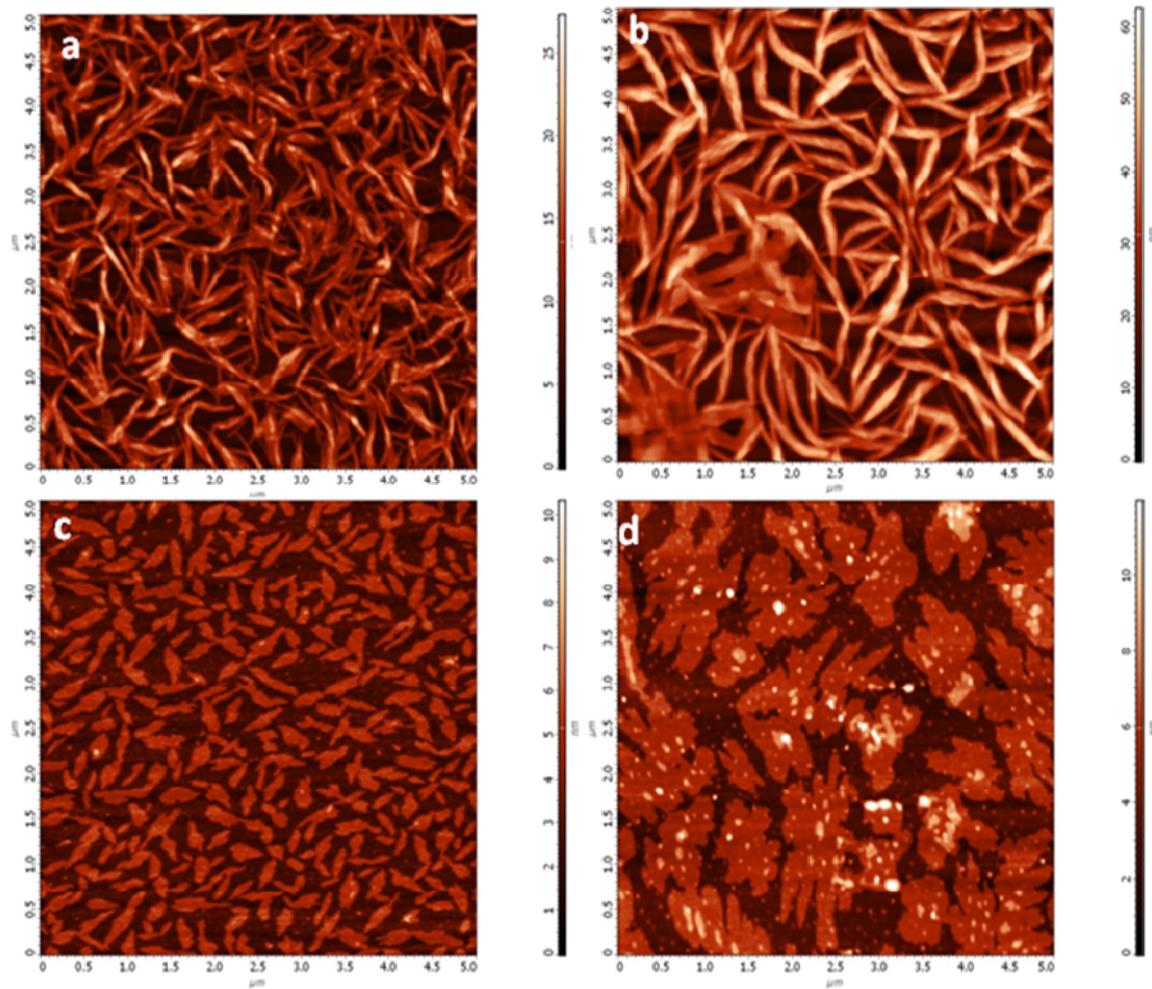


Figure S6. AFM images of **6F** after deposition times of (a) 20 s, (b) 60 s, and of **DH6F** after deposition times of (c) 30 s and (d) 60 s, on OTS-functionalized Si/SiO₂.

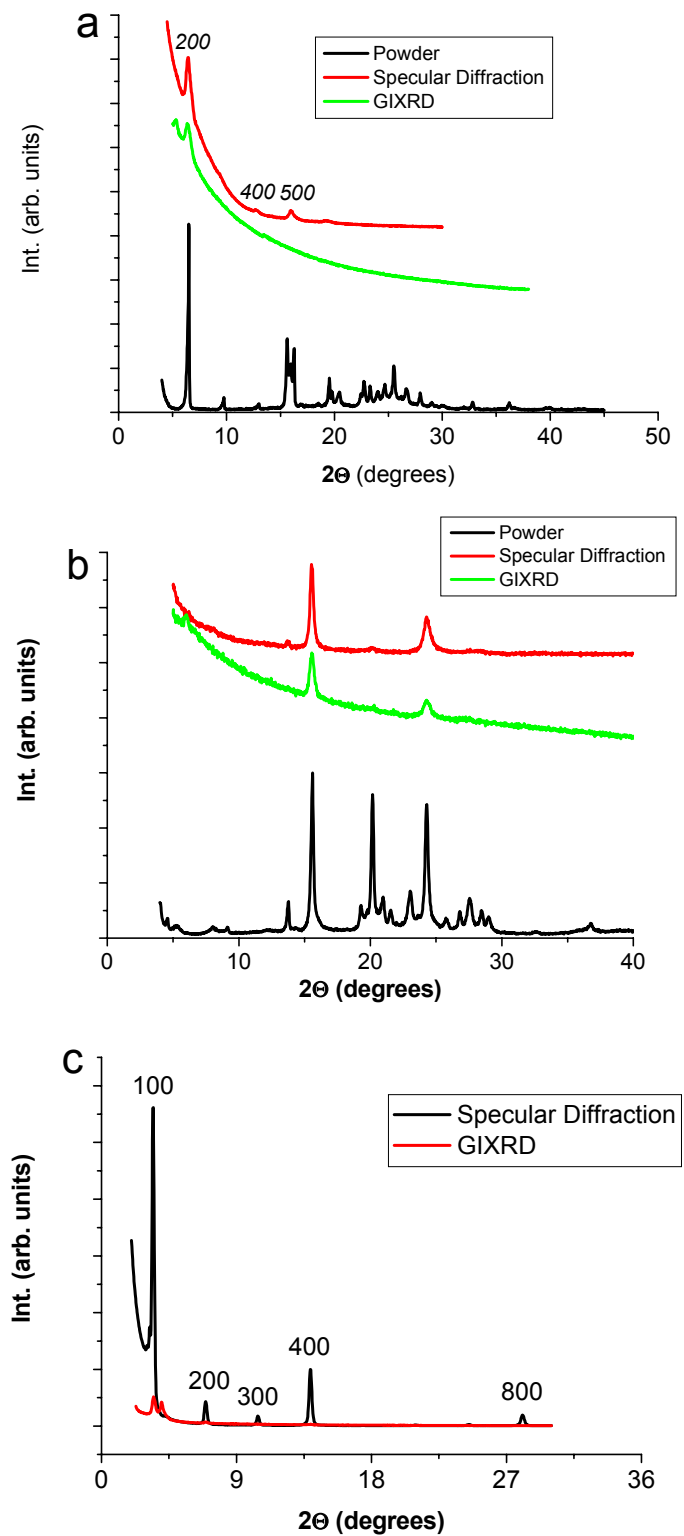


Figure S7. XRD patterns for vacuum deposited films of (a) **DH6F** (b) **6F**, and (c) **8F**.

Electrochemistry

All electrochemical measurements were performed using PAR Potentiostat model 263A in a standard three-electrode, one compartment configuration equipped with Ag/AgCl wire, Pt wire, and Pt disk electrode (dia. 1.6 mm from BASi) as the pseudo reference, counter electrode, and working electrode, respectively. Pt disk electrodes were polished with alumina followed by sonication and further electropolished in 0.5 M HClO₄ by cycling between -0.23 and 1.25 V vs. Ag/AgCl saturated NaCl electrode (BASi). The electrolytic medium contained anhydrous dichloroethane (DCE) and 0.1 M TBABF₄ as electrolyte. All electrochemical solutions were purged with dry N₂ for at least 15 minutes. Under these conditions, a Fc/Fc⁺ standard was calibrated to be 0.4 V vs. SCE.³

	E_{pa} (V)	E_{pc} (V)
6F	0.72	0.48
DH-6F	0.69	0.58
DH-6T	0.97	-

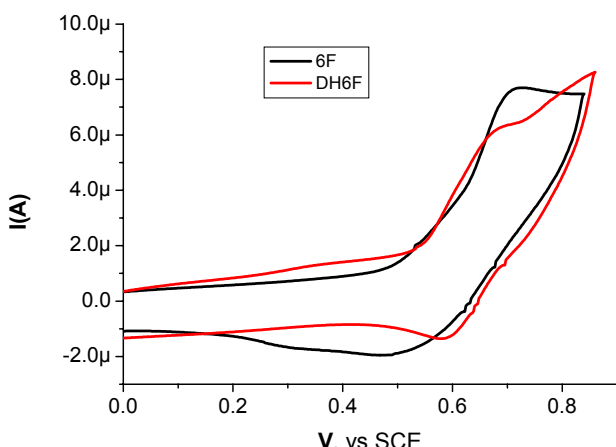


Figure S8. (a) CV of **6F** and **DH-6F** in DCE with 0.1 M TBABF₄ (scan rate 100 mV/s). Fc/Fc⁺ = 0.40 V vs. SCE under these conditions.

Device Fabrication and Testing. Thin film transistors (OTFTs) were fabricated in both bottom- and top-contact configurations using 190 nm-thick SiO₂ as the dielectric, which was thermally grown on a heavily n-doped (Sb, $\rho \sim 0.01\text{--}0.02$ Ohm cm) silicon substrate. In the bottom-contact configuration, 25 nm Au electrodes were patterned by the lift off technique and using a 5 nm thick Cr adhesion layer, while in the top-contact configuration, Au electrodes were deposited using a shadow mask.

Prior to deposition, substrates were cleaned by sonication in acetone and isopropyl alcohol followed by plasma cleaning. The bottom-contact devices had channel lengths of 6 μm and corresponding widths of 1880 μm and the top-contact devices had channel lengths of 50, 100 μm

and widths of 500, 1000 μm . The films of each compound were deposited on hexamethyldisilazane (HMDS) treated substrates by vacuum sublimation (ultimate pressure $\sim 10^{-6}$ Torr) at a deposition rate of 0.1 to 0.3 \AA s^{-1} until a nominal thickness of about 50 nm was reached.

The charge carrier mobilities of OTFTs were calculated in the saturation regime from a plot of the square root of the drain current vs. gate voltage using the following equation:

$$I_{DS} = C_i \mu (W / 2L)(V_G - V_T)^2$$

where I_{DS} is the drain-source current, C_i is the capacitance per unit area of the gate dielectric (18 nF/cm^2), L is the channel length, W is the channel width, and V_T and V_G are the threshold voltage and gate voltage, respectively. Electrical measurements were carried out at room temperature and under vacuum using a semiconductor parameter analyzer (Keithley 4200).

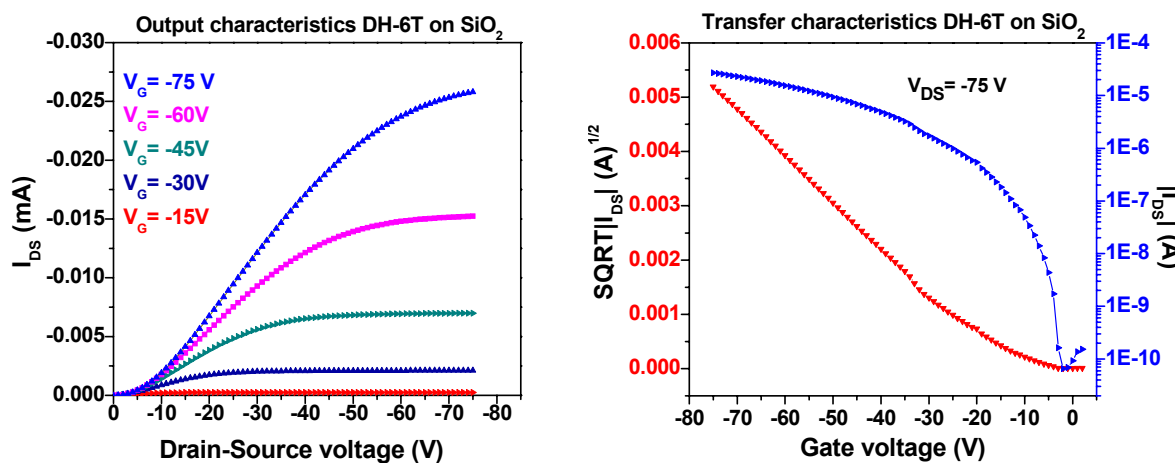


Figure S9. Output (left) and transfer curves (right) of top-contact OFET ($W/L = 1000/50 \mu\text{m}$) based on a vacuum sublimed film ($\sim 50 \text{ nm}$) of **DH-6T** (at room temperature).

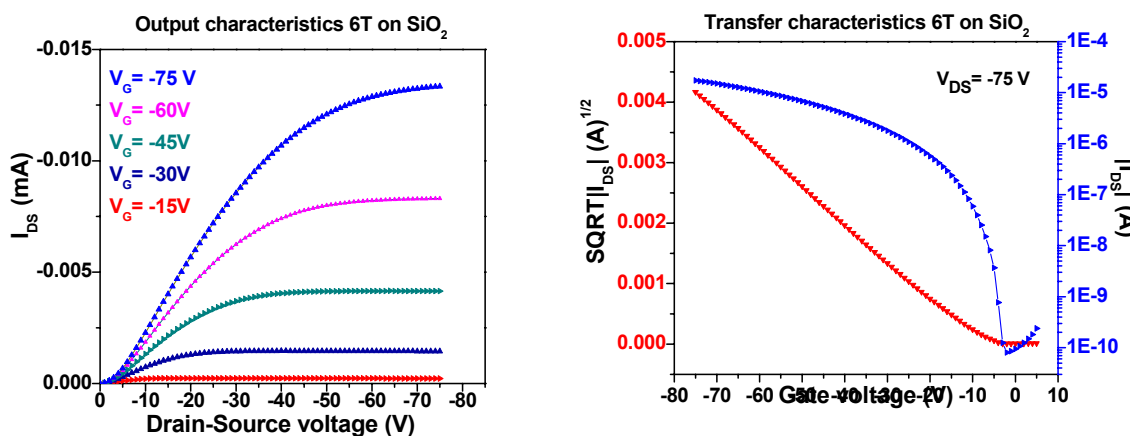


Figure S10. Output (left) and transfer curves (right) of top-contact TFT ($W/L = 1000/50 \mu\text{m}$) based on a vacuum sublimed film ($\sim 50 \text{ nm}$) of **6T** (at room temperature).

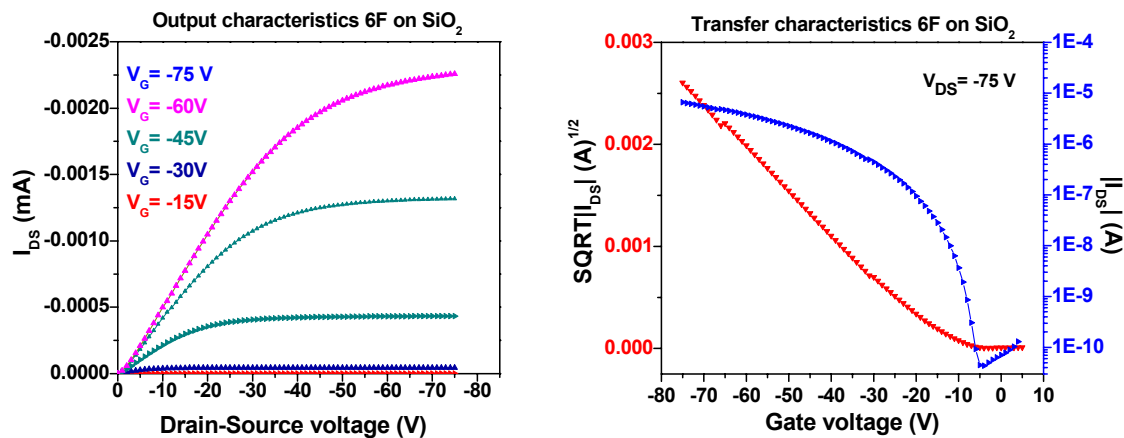


Figure S11. Output (left) and transfer curves (right) of bottom-contact TFT (W/L= 1880/6 μm) based on a vacuum sublimed film (~50 nm) of 6F (at room temperature).

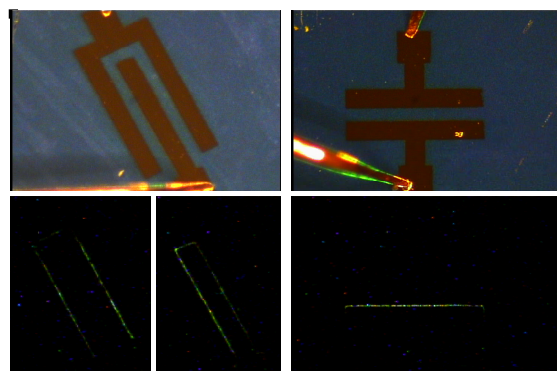


Figure S12. Electroluminescence of a top-contact OFET based on DH6F. (W/L= 1000/50 and 500/50 μm). The top images show the device under external illumination. The bottom images show electroluminescence appearing in the vicinity of the cathode upon biasing of the gated device.

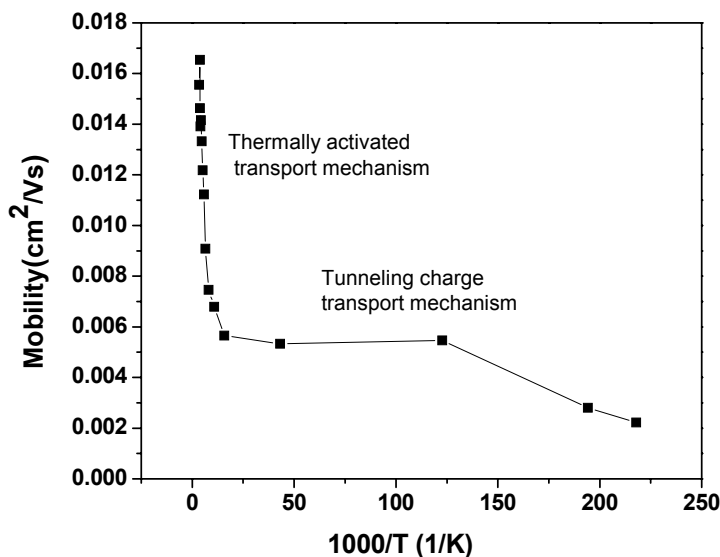


Figure S13. Hole mobility measurements in OFET based on **DH6F** measured as a function of temperature in the 4.6–300 K range. Below ~50 K, tunneling (band-like transport) is a dominant charge transport mechanism and the mobility becomes almost temperature independent.⁷ At higher temperatures, thermally activated hopping becomes the dominant means of charge transport. Analysis of the slope of the Arrhenius logarithmic plot, $\mu_{\text{eff}} \sim \exp(-E_a/kT)$ (E_a , k , and T are the activation energy, Boltzmann constant, and temperature, respectively)⁵ gives an activation energy of ~14 meV. **DH6T** OFETs showed very similar value activation energy (17meV) although 2-3 times higher values were previously reported^{6,7} for this material.

Details of computations. All calculations were carried out using the Gaussian 03 program.⁸ All molecules were optimized using a hybrid density functional⁹ and Becke's three-parameter exchange functional combined with the LYP correlation functional (B3LYP)¹⁰ and with the 6-31G(d) basis set (B3LYP/6-31G(d)). Some results for oligofurans and oligothiophenes were taken from reference 11. The B3LYP/6-31G(d) level is currently widely used to study organic electronic materials and conducting polymers because it predicts geometries very reliably and provides good estimates for HOMO–LUMO gaps.^{11,12,13} The length of **DH-6F** and **8F** were calculated by taking the molecular length of the optimized structure at B3LYP/6-31G(d) and adding the van der Waals (VDW) radii of the methyl group (0.2 nm) for DH-6F or VDW of hydrogen (0.12 nm) for **8F**. Calculations of orbitals splitting were performed using the geometries obtained from X-ray measurements. Positions of hydrogen atoms were optimized at B3LYP/6-31G(d) while constraining the positions of all other atoms. Two possible dimer structures were considered for **6F** and **6T**, however only one structure was found to contribute significantly to orbital splitting. For similar previous estimations of reorganization energies based on similar calculations of orbital splitting see reference 14.

Table S1. Calculated (B3LYP/6-31G(d)) frontier orbitals, orbital energy splittings, and absolute energies for different **6F** and **6T** dimers.

	6F conf.1	6F conf.2	6T conf.1	6T conf.2
HOMO -1 (eV)	-4.69	-4.64	-4.92	-4.80
HOMO (eV)	-4.38	-4.53	-4.56	-4.77
LUMO (eV)	-1.64	-1.55	-2.20	-2.16
LUMO +1 (eV)	-1.30	-1.48	-1.84	-1.95
HOMO-(HOMO-1) (eV)	0.31	0.11	0.36	0.02
LUMO-(LUMO-1) (eV)	0.34	0.07	0.36	0.20
LUMO-HOMO (eV)	2.74	2.97	2.36	2.62
Absolute Energies (Hartree)	-2748.4328582	-2748.4360475	-6624.1378678	-6624.1412915

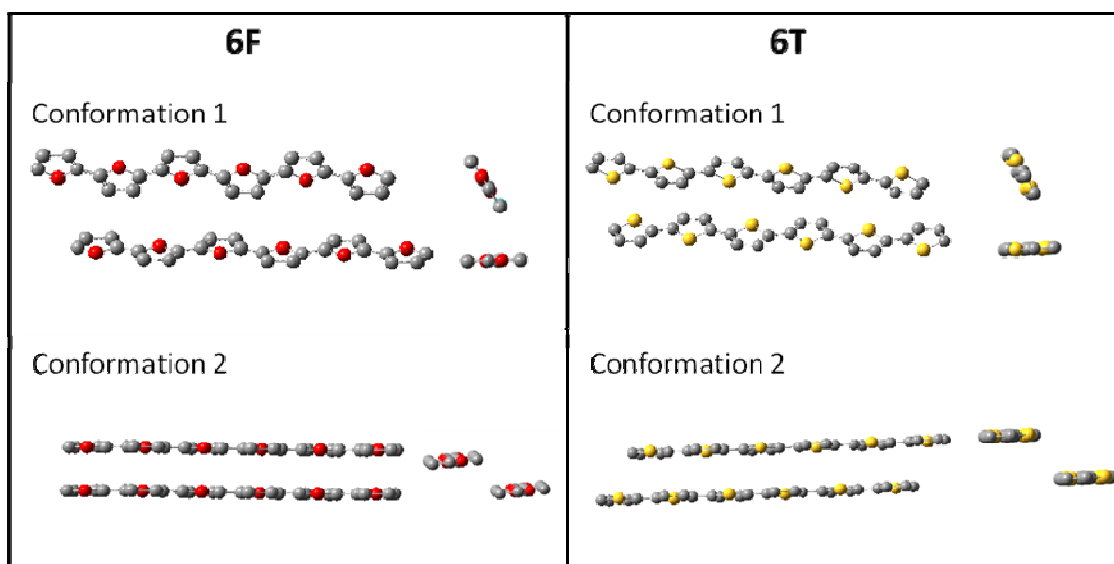


Figure S14. Calculated (B3LYP/6-31G(d)) dimer structures for **6F** (left) and **6T** (right), hydrogens omitted for clarity.

Cartesian coordinates of **6F** and **6T** dimers calculated at B3LYP/6-31G(d).

6F Conformation 1

Center Number	Atomic Number	Atomic Type	Coordinates (Angstroms)		
			X	Y	Z
1	8	0	-2.942651	1.661825	-0.329009
2	8	0	-6.475662	2.265530	0.109381
3	8	0	-9.845184	1.010028	-0.193828
4	6	0	-1.908938	2.521254	-0.017401
5	6	0	-2.399195	3.675903	0.502510
6	6	0	-3.800400	3.543451	0.517138
7	6	0	-4.106583	2.320108	0.002346
8	6	0	-5.310935	1.607000	-0.230438
9	6	0	-5.599034	0.373322	-0.739577
10	6	0	-7.016966	0.251316	-0.725258
11	6	0	-7.495741	1.410954	-0.205198
12	6	0	-8.820770	1.874288	0.088768
13	6	0	-9.308286	3.026959	0.587612
14	6	0	-10.721310	2.892750	0.638388
15	6	0	-10.997717	1.670219	0.156775
16	8	0	0.440643	2.883101	0.026141
17	8	0	3.973653	2.279396	-0.412249
18	8	0	7.343176	3.534898	-0.109039
19	6	0	-0.593072	2.023673	-0.285467
20	6	0	-0.102815	0.869022	-0.805376
21	6	0	1.298390	1.001475	-0.820006
22	6	0	1.604573	2.224819	-0.305213
23	6	0	2.808925	2.937926	-0.072430
24	6	0	3.097025	4.171603	0.436709
25	6	0	4.514955	4.293610	0.422389
26	6	0	4.993731	3.133971	-0.097669
27	6	0	6.318760	2.670638	-0.391636
28	6	0	6.806276	1.517966	-0.890480
29	6	0	8.219301	1.652176	-0.941256
30	6	0	8.495708	2.874707	-0.459643
31	8	0	-0.479873	-2.349604	0.665434
32	8	0	6.436479	-1.732679	0.581355
33	8	0	-7.380695	-3.024654	0.770474
34	6	0	1.883154	-2.170540	0.472053
35	6	0	2.271254	-1.936555	1.752094
36	6	0	3.673028	-1.811853	1.727418
37	6	0	4.081559	-1.979728	0.438912
38	6	0	-2.834614	-2.588504	0.525409
39	6	0	-3.225300	-2.427734	1.823755
40	6	0	-4.643183	-2.550386	1.837237
41	6	0	-5.019563	-2.782612	0.553159

42	6	0	8.795034	-1.524222	0.365044
43	6	0	9.182008	-1.310218	1.637686
44	6	0	10.593084	-1.149528	1.621235
45	6	0	10.969557	-1.287212	0.339734
46	8	0	2.981916	-2.195317	-0.362446
47	8	0	-3.934437	-2.812243	-0.278370
48	8	0	9.882738	-1.520268	-0.467492
49	6	0	0.618889	-2.374382	-0.169065
50	6	0	0.230789	-2.608367	-1.449105
51	6	0	-1.170986	-2.733068	-1.424430
52	6	0	-1.579517	-2.565193	-0.135923
53	6	0	5.336657	-1.956418	-0.222423
54	6	0	5.727342	-2.117187	-1.520770
55	6	0	7.145225	-1.994534	-1.534252
56	6	0	7.521606	-1.762309	-0.250174
57	6	0	-6.292991	-3.020700	-0.062062
58	6	0	-6.679965	-3.234704	-1.334705
59	6	0	-8.091042	-3.395394	-1.318253
60	6	0	-8.467515	-3.257709	-0.036752
61	1	0	-9.418073	-3.292618	0.472931
62	1	0	-1.813926	4.520939	0.834612
63	1	0	-4.519159	4.272908	0.863568
64	1	0	-4.878491	-0.353108	-1.083594
65	1	0	-7.608443	-0.589612	-1.053262
66	1	0	-8.720612	3.881360	0.891916
67	1	0	-11.435516	3.625683	0.987255
68	1	0	-11.910539	1.117143	-0.003917
69	1	0	-0.687591	0.027739	-1.144094
70	1	0	2.016278	0.271658	-1.164990
71	1	0	2.375211	4.896990	0.782779
72	1	0	5.108241	5.135516	0.747856
73	1	0	6.219512	0.666850	-1.201872
74	1	0	8.931851	0.917392	-1.287073
75	1	0	9.408014	3.428133	-0.297188
76	1	0	1.618179	-1.858509	2.608848
77	1	0	4.323520	-1.620068	2.569116
78	1	0	-2.571622	-2.235053	2.661764
79	1	0	-5.303680	-2.478173	2.688670
80	1	0	8.527768	-1.262927	2.496476
81	1	0	11.239288	-0.960071	2.466944
82	1	0	11.920222	-1.252658	-0.170083
83	1	0	0.882936	-2.686859	-2.306868
84	1	0	-1.821267	-2.924887	-2.266603
85	1	0	5.073980	-2.309785	-2.359313
86	1	0	7.804564	-2.067510	-2.386850
87	1	0	-6.026705	-3.284204	-2.194481
88	1	0	-8.737096	-3.586684	-2.163836

6F Conformation 2

Center Number	Atomic Number	Atomic Type	Coordinates (Angstroms)		
			X	Y	Z
1	8	0	2.540268	-1.197690	0.259025
2	8	0	5.788271	-1.197690	-1.318722
3	8	0	8.513568	0.730280	-2.688973
4	6	0	1.817114	-2.298923	0.669653
5	6	0	2.504917	-3.438612	0.401494
6	6	0	3.710847	-3.042893	-0.207006
7	6	0	3.706828	-1.683312	-0.289773
8	6	0	4.616644	-0.709214	-0.776129
9	6	0	4.600099	0.654457	-0.841802
10	6	0	5.820164	1.043956	-1.462570
11	6	0	6.498222	-0.102668	-1.727031
12	6	0	7.783323	-0.364020	-2.307554
13	6	0	8.457863	-1.495495	-2.590268
14	6	0	9.692640	-1.107701	-3.175221
15	6	0	9.680356	0.234300	-3.217853
16	8	0	0.169852	3.113890	-1.690022
17	8	0	3.417855	3.113890	-3.267768
18	8	0	6.143152	5.041861	-4.638020
19	6	0	-0.553303	2.012658	-1.279393
20	6	0	0.134500	0.872968	-1.547553
21	6	0	1.340431	1.268687	-2.156052
22	6	0	1.336411	2.628269	-2.238819
23	6	0	2.246227	3.602366	-2.725175
24	6	0	2.229683	4.966037	-2.790849
25	6	0	3.449747	5.355536	-3.411616
26	6	0	4.127805	4.208912	-3.676078
27	6	0	5.412906	3.947560	-4.256600
28	6	0	6.087446	2.816085	-4.539315
29	6	0	7.322224	3.203879	-5.124268
30	6	0	7.309940	4.545880	-5.166900
31	8	0	-0.169852	-3.113890	1.690022
32	8	0	-3.417855	-3.113890	3.267768
33	8	0	-6.143152	-5.041861	4.638020
34	6	0	0.553303	-2.012658	1.279393
35	6	0	-0.134500	-0.872968	1.547553
36	6	0	-1.340431	-1.268687	2.156052
37	6	0	-1.336411	-2.628269	2.238819
38	6	0	-2.246227	-3.602366	2.725175
39	6	0	-2.229683	-4.966037	2.790849
40	6	0	-3.449747	-5.355536	3.411616
41	6	0	-4.127805	-4.208912	3.676078

42	6	0	-5.412906	-3.947560	4.256600
43	6	0	-6.087446	-2.816085	4.539315
44	6	0	-7.322224	-3.203879	5.124268
45	6	0	-7.309940	-4.545880	5.166900
46	8	0	-2.540268	1.197690	-0.259025
47	8	0	-5.788271	1.197690	1.318722
48	8	0	-8.513568	-0.730280	2.688973
49	6	0	-1.817114	2.298923	-0.669653
50	6	0	-2.504917	3.438612	-0.401494
51	6	0	-3.710847	3.042893	0.207006
52	6	0	-3.706828	1.683312	0.289773
53	6	0	-4.616644	0.709214	0.776129
54	6	0	-4.600099	-0.654457	0.841802
55	6	0	-5.820164	-1.043956	1.462570
56	6	0	-6.498222	0.102668	1.727031
57	6	0	-7.783323	0.364020	2.307554
58	6	0	-8.457863	1.495495	2.590268
59	6	0	-9.692640	1.107701	3.175221
60	6	0	-9.680356	-0.234300	3.217853
61	1	0	2.176915	-4.444302	0.620402
62	1	0	4.505106	-3.687748	-0.556267
63	1	0	3.805341	1.296991	-0.494290
64	1	0	6.154351	2.046368	-1.682894
65	1	0	8.113340	-2.501258	-2.395901
66	1	0	10.484619	-1.757351	-3.521073
67	1	0	10.380818	0.979822	-3.562058
68	1	0	-0.190126	-0.133085	-1.328645
69	1	0	2.132719	0.621941	-2.503738
70	1	0	1.433041	5.606527	-2.441479
71	1	0	3.788082	6.357724	-3.630345
72	1	0	5.746433	1.810118	-4.343458
73	1	0	8.113045	2.550913	-5.465493
74	1	0	8.007677	5.291765	-5.515901
75	1	0	0.190126	0.133085	1.328645
76	1	0	-2.132719	-0.621941	2.503738
77	1	0	-1.433041	-5.606527	2.441479
78	1	0	-3.788082	-6.357724	3.630345
79	1	0	-5.746433	-1.810118	4.343458
80	1	0	-8.113045	-2.550913	5.465493
81	1	0	-8.007677	-5.291765	5.515901
82	1	0	-2.176915	4.444302	-0.620402
83	1	0	-4.505106	3.687748	0.556267
84	1	0	-3.805341	-1.296991	0.494290
85	1	0	-6.154351	-2.046368	1.682894
86	1	0	-8.113340	2.501258	2.395901
87	1	0	-10.484619	1.757351	3.521073
88	1	0	-10.380818	-0.979822	3.562058

6T conformation 1

Center Number	Atomic Number	Atomic Type	Coordinates (Angstroms)		
			X	Y	Z
1	16	0	-2.638137	1.359715	-0.490783
2	16	0	-6.604986	3.075710	0.223166
3	6	0	-1.440462	2.538370	-0.072168
4	6	0	-2.033970	3.686678	0.373032
5	6	0	-3.436415	3.641779	0.373741
6	6	0	-3.930554	2.437712	-0.074069
7	6	0	-5.300850	2.011793	-0.202911
8	6	0	-7.798945	1.885549	-0.188673
9	6	0	-9.205917	2.172570	-0.071651
10	6	0	-9.829528	3.351204	0.361601
11	6	0	-11.239515	3.227338	0.353491
12	6	0	-11.677390	2.023872	-0.059453
13	16	0	-10.384155	0.979744	-0.458381
14	6	0	-5.792649	0.814096	-0.649052
15	6	0	-7.195190	0.737566	-0.650565
16	16	0	-8.955551	-2.924948	-0.923868
17	16	0	-5.097843	-2.492502	1.097288
18	6	0	-10.191276	-2.859624	0.254261
19	6	0	-9.704341	-2.695810	1.493996
20	6	0	-8.298758	-2.616152	1.526130
21	6	0	-7.719338	-2.734634	0.270379
22	16	0	8.923161	3.730311	0.294687
23	16	0	5.130425	1.682717	-0.464585
24	16	0	1.166693	3.406286	0.229558
25	6	0	10.199085	2.665719	-0.102729
26	6	0	7.726498	2.556808	-0.131412
27	6	0	6.324851	2.863109	-0.025715
28	6	0	5.722309	4.003458	0.419971
29	6	0	4.318362	3.947540	0.405377
30	6	0	3.831185	2.758488	-0.050369
31	6	0	2.458424	2.333270	-0.189665
32	6	0	-0.035211	2.229581	-0.191443
33	6	0	9.753289	1.479141	-0.543397
34	6	0	8.347812	1.397007	-0.573610
35	6	0	1.964853	1.139197	-0.643843
36	6	0	0.565702	1.075446	-0.649581
37	16	0	-1.201022	-2.552693	-0.896419
38	16	0	2.670223	-2.157134	1.113826
39	16	0	6.571305	-2.238192	-0.877467
40	16	0	10.420917	-1.893411	1.172244
41	6	0	-6.331670	-2.693417	-0.106827
42	6	0	-5.769871	-2.820884	-1.343856

43	6	0	-4.366522	-2.750127	-1.340856
44	6	0	-3.838748	-2.570247	-0.096666
45	6	0	-2.452953	-2.469049	0.295783
46	6	0	-1.918493	-2.291558	1.544199
47	6	0	-0.519187	-2.231514	1.552828
48	6	0	0.040778	-2.367829	0.299490
49	6	0	1.432448	-2.338996	-0.083564
50	6	0	1.984817	-2.464529	-1.327837
51	6	0	3.386712	-2.406028	-1.339174
52	6	0	3.922494	-2.237106	-0.082628
53	6	0	5.306271	-2.146335	0.308061
54	6	0	5.839456	-1.977591	1.558107
55	6	0	7.242949	-1.924552	1.577967
56	6	0	7.806204	-2.065845	0.329572
57	6	0	9.200588	-2.039980	-0.031905
58	6	0	9.781025	-2.145128	-1.303851
59	6	0	11.194040	-2.096706	-1.236792
60	6	0	11.675003	-1.964249	0.012903
61	1	0	-11.225630	-2.947714	-0.051113
62	1	0	-10.327993	-2.626839	2.378941
63	1	0	-7.719511	-2.478139	2.432824
64	1	0	-6.354769	-2.965687	-2.246647
65	1	0	-3.762648	-2.833503	-2.238433
66	1	0	-2.524961	-2.204385	2.439540
67	1	0	0.070582	-2.090771	2.452212
68	1	0	1.389688	-2.597256	-2.225895
69	1	0	3.987718	-2.487041	-2.238303
70	1	0	5.229660	-1.887162	2.451140
71	1	0	7.826467	-1.787210	2.481624
72	1	0	9.209716	-2.252293	-2.218602
73	1	0	11.831561	-2.162714	-2.112997
74	1	0	12.707614	-1.904436	0.329850
75	1	0	-12.699031	1.682092	-0.158692
76	1	0	-11.906775	4.030083	0.651984
77	1	0	-9.288228	4.240523	0.662623
78	1	0	-7.749375	-0.133570	-0.977772
79	1	0	-5.154846	0.001491	-0.978534
80	1	0	-4.067890	4.463919	0.692528
81	1	0	-1.466813	4.554749	0.694024
82	1	0	0.004083	0.210687	-0.981444
83	1	0	2.599836	0.324240	-0.971973
84	1	0	3.684149	4.767500	0.725917
85	1	0	6.279527	4.872876	0.754240
86	1	0	7.797760	0.524683	-0.904763
87	1	0	10.405091	0.668633	-0.848982
88	1	0	11.224105	2.991154	0.018703

6T conformation 2

Center Number	Atomic Number	Atomic Type	Coordinates (Angstroms)		
			X	Y	Z
1	16	0	3.313801	1.555754	-0.628685
2	16	0	7.350108	2.985452	0.295678
3	6	0	2.168531	2.728152	-0.069463
4	6	0	2.811333	3.788738	0.505889
5	6	0	4.209607	3.672160	0.516226
6	6	0	4.650626	2.504829	-0.064570
7	6	0	6.001217	2.039574	-0.252082
8	6	0	8.491917	1.810618	-0.276743
9	6	0	9.908541	2.001805	-0.097102
10	6	0	10.581119	3.071931	0.509730
11	6	0	11.984894	2.895574	0.467469
12	6	0	12.372141	1.757984	-0.137937
13	16	0	11.036309	0.844779	-0.688768
14	6	0	6.440129	0.877882	-0.829330
15	6	0	7.837777	0.738513	-0.841029
16	16	0	-8.123672	4.440301	0.245328
17	16	0	-11.044612	-0.820663	0.618364
18	16	0	-4.428287	2.273495	-0.650813
19	16	0	-7.349228	-2.987470	-0.277773
20	16	0	-0.396285	3.693767	0.292312
21	16	0	-3.317226	-1.567200	0.665355
22	16	0	0.392862	-3.705213	-0.255642
23	16	0	4.429167	-2.275515	0.668719
24	6	0	-9.442504	3.513465	-0.321186
25	6	0	-12.363442	-1.747503	0.051865
26	6	0	-6.979821	3.265860	-0.305097
27	6	0	-9.900764	-1.995106	0.067951
28	6	0	-5.568922	3.461867	-0.103723
29	6	0	-8.489864	-1.799099	0.269322
30	6	0	-4.917220	4.516933	0.465671
31	6	0	-7.838158	-0.744030	0.838721
32	6	0	-3.518676	4.381554	0.478080
33	6	0	-6.439619	-0.879411	0.851136
34	6	0	-3.084864	3.218806	-0.086470
35	6	0	-6.005802	-2.042159	0.286578
36	6	0	-1.732504	2.746118	-0.266401
37	6	0	-4.653441	-2.514848	0.106647
38	6	0	0.753079	2.520640	-0.263733
39	6	0	-2.167863	-2.740324	0.109312
40	6	0	-0.752410	-2.532813	0.303582
41	6	0	-0.109605	-1.472223	0.878937
42	6	0	1.288664	-1.588805	0.889282
43	6	0	1.729688	-2.756136	0.308478

44	6	0	3.080280	-3.221391	0.120964
45	6	0	5.570977	-3.450348	0.096303
46	6	0	6.987600	-3.259161	0.275945
47	6	0	7.660185	-2.189026	0.882779
48	6	0	9.063950	-2.365390	0.840524
49	6	0	9.451204	-3.502982	0.235112
50	16	0	8.115370	-4.416185	-0.315732
51	6	0	-9.048913	2.366118	-0.895269
52	6	0	-11.969856	-2.894849	-0.522214
53	6	0	-7.650369	2.201545	-0.891877
54	6	0	-10.571301	-3.059407	-0.518830
55	6	0	-1.292299	1.580781	-0.835532
56	6	0	-4.213243	-3.680185	-0.462477
57	6	0	0.101914	1.447029	-0.835013
58	6	0	-2.819022	-3.813932	-0.461963
59	6	0	3.519185	-4.383084	-0.456272
60	6	0	4.916840	-4.522450	-0.467980
61	1	0	13.378231	1.393392	-0.296529
62	1	0	12.685315	3.611759	0.885710
63	1	0	10.077839	3.923437	0.952560
64	1	0	8.350256	-0.122295	-1.254290
65	1	0	5.766912	0.130800	-1.236619
66	1	0	4.875474	4.419273	0.934097
67	1	0	2.283455	4.642279	0.919347
68	1	0	0.621596	0.588497	-1.244655
69	1	0	-1.962402	0.833872	-1.247765
70	1	0	-2.850039	5.128408	0.893199
71	1	0	-5.434324	5.380474	0.871715
72	1	0	-7.141758	1.339240	-1.307722
73	1	0	-9.735644	1.638772	-1.314788
74	1	0	-10.451075	3.884049	-0.192154
75	1	0	10.457086	-3.868550	0.077552
76	1	0	9.763783	-1.648367	1.257500
77	1	0	7.159102	-1.337561	1.326193
78	1	0	5.431889	-5.381938	-0.883189
79	1	0	2.844705	-5.128973	-0.864621
80	1	0	1.953414	-0.841060	1.307023
81	1	0	-0.635526	-0.618702	1.292472
82	1	0	-2.297456	-4.672402	-0.871788
83	1	0	-4.884417	-4.426544	-0.874786
84	1	0	-5.772210	-0.131233	1.264937
85	1	0	-8.352842	0.120586	1.243217
86	1	0	-10.060483	-3.921700	-0.934094
87	1	0	-12.657059	-3.621440	-0.943098
88	1	0	-13.372229	-1.377785	0.181832

References

- 1 Lakowicz, J. R., *Principles of Fluorescence spectroscopy*. 2nd ed., Kluwer Academic/Plenum: New York, 1999
- 2 Jones, G., Jackson, W. R., Choi, C., Bergmark, W. R. *J. Phys. Chem.*, 1985, **89**, 294-300.
- 3 Eugster, N., Fermⁿ, D. J., Girault, H. H. *J. Phys. Chem. B*, 2002, **106**, 3428-3433.
- 4 Gidron, O., Diskin-Posner, Y., Bendikov, M. *J. Am. Chem. Soc.*, 2010, **132**, 2148.
- ⁵ T. Minari, T. Nemoto, and S. Isoda, *J. Appl. Phys.*, 2006, **99**, 034506.
- ⁶ H.Seo, Y. Zhang, Y. Jang, and J. Choi, *Appl. Phys. Lett.* 2008, **92**, 223310.
- ⁷ G. Horowitz, R. Hajlaoui, R. Bourguiga, and M. Hajlaoui, *Synth. Met.*, 1999, **101**, 401.
- 8 Frisch, M. J., Trucks, G. W., Schlegel, H. B., Scuseria, G. E., Robb, M. A., Cheeseman, J. R., Montgomery, J. A., Jr., Vreven, T., Kudin, K. N., Burant, J. C., Millam, J. M., Iyengar, S. S., Tomasi, J., Barone, V., Mennucci, B., Cossi, M., Scalmani, G., Rega, N., Petersson, G. A., Nakatsuji, H., Hada, M., Ehara, M., Toyota, K., Fukuda, R., Hasegawa, J., Ishida, M., Nakajima, T., Honda, Y., Kitao, O., Nakai, H., Klene, M., Li, X., Knox, J. E., Hratchian, H. P., Cross, J. B., Adamo, C., Jaramillo, J., Gomperts, R., Stratmann, R. E., Yazyev, O., Austin, A. J., Cammi, R., Pomelli, C., Ochterski, J. W., Ayala, P. Y., Morokuma, K., Voth, G. A., Salvador, P., Dannenberg, J. J., Zakrzewski, V. G., Dapprich, S., Daniels, A. D., Strain, M. C., Farkas, O., Malick, D. K., Rabuck, A. D., Raghavachari, K., Foresman, J. B., Ortiz, J. V., Cui, Q., Baboul, A. G., Clifford, S., Cioslowski, J., Stefanov, B. B., Liu, G., Liashenko, A., Piskorz, P., Komaromi, I., Martin, R. L., Fox, D. J., Keith, T., Al-Laham, M. A., Peng, C. Y., Nanayakkara, A., Challacombe, M., Gill, P. M. W., Johnson, B., Chen, W., Wong, M. W., Gonzalez, C., Pople, J. A., *Gaussian 03*, Revision C.02, Gaussian, Inc.: Wallingford CT, 2004.
- 9 (a) Parr, R. G., Yang, W. *Density-functional Theory of Atoms and Molecules*, Oxford University Press, New York, 1989. (b) Koch, W., Holthausen, M. C. *A Chemist's Guide to Density Functional Theory*, Wiley-VCH, New York, 2000.
- 10 (a) Lee, C., Yang, W., Parr, R. G. *Phys. Rev. B*, 1988, **37**, 785. (b) Becke, A. D. *J. Chem. Phys.*, 1993, **98**, 5648.
- 11 Zade, S. S., Bendikov, M. *Org. Lett.*, 2006, **8**, 5243-46.
- 12 Zade, S. S., Bendikov, M. *J. Phys. Chem. B*, 2006, **110**, 15839-15846.
- 13 (a) Johansson T., Mammo W., Svensson M., Anderssonb M. R., Inganas O. *J. Mater. Chem.*, 2003, **13**, 1316. (b) Hutchison G. R., Ratner M. A., Marks T. J., *J. Phys. Chem. B*, 2005, **109**, 3126. (c) Hutchison G. R., Ratner M. A., Marks T. J. *J. Phys. Chem. A*, 2002, **106**, 10596. (d) Yang S., Olshevski P., Kertesz M. *Synth. Met.*, 2004, **141**, 171. (e) Zhan C .G., Nichols J. A., Dixon D. A., *J. Phys. Chem. A*, 2003, **107**, 4184. (f) Stowasser R., Hoffmann R. *J. Am. Chem. Soc.*, 1999, **121**, 3414. (g) Baerends E. J., Gritsenko O. V. *J. Phys. Chem. A*, 1997, **101**, 5383.
- 14 (a) Brédas, J. L., Calbert, J. P., da Silva, D. A., Cornil, J. *Proc. Natl. Acad. Sci., U.S.A.* 2002, **99**, 5804. (b) Hutchison, G. R., Ratner, M. A., Marks, T. J. *J. Am. Chem. Soc.*, 2005, **127**, 16866.